Biogeosciences Discuss., 7, 921–952, 2010
www.biogeosciences-discuss.net/7/921/2010/

Biogeosciences Discussions

This discussion paper is/has been under review for the journal Biogeosciences (BG).
Please refer to the corresponding final paper in BG if available.

Sensitivity of Holocene atmospheric CO_2 and the modern carbon budget to early human land use: analyses with a process-based model

B. Stocker[1,2], **K. Strassmann**[1,2,*], **and F. Joos**[1,2]

[1]Climate and Environmental Physics, Physics Institute, University of Bern, Switzerland
[2]Oeschger Centre for Climate Change Research, University of Bern, Switzerland
[*]now at: National Institute for Environmental Sciences, Center for Global Environmental Research, Tsukuba-City, Japan

Received: 28 January 2010 – Accepted: 1 February 2010 – Published: 5 February 2010

Correspondence to: B. Stocker (beni@climate.unibe.ch)

Published by Copernicus Publications on behalf of the European Geosciences Union.

Abstract

A Dynamic Global Vegetation model is used as part of a simplified Earth system model to simulate the impact of human land use on Holocene atmospheric CO_2 and the contemporary carbon cycle. We show that suggested upward revisions of Holocene land use reconstructions imply a smaller contemporary terrestrial carbon sink and that early agricultural activities did only marginally contribute to the late Holocene CO_2 rise of 20 ppm measured on ice cores. Scenarios are used to test the robustness of the results. Simulated changes in atmospheric CO_2 due to land use are less than 1 ppm before 0 AD and 22 ppm by 2004 AD when prescribing the HYDE 3.1 land use reconstruction over the past 12 000 years. Cumulative emissions are with 50 GtC by 1850 and 177 GtC by 2004 AD comparable to earlier estimates. In scenario H2, agricultural area from HYDE 3.1 is scaled by a factor of two before 1700 AD, thereby taking into account evidence that land area used per person was higher before than during early industrialisation. Then, the contemporary terrestrial carbon sink, required to close the atmospheric CO_2 budget, is reduced by 0.5 GtC yr^{-1}. CO_2 changes due to land use change exceed natural interannual variability only after 1000 AD and are less than 4 ppmv until 1850 AD. Simulated CO_2 change remains small even in scenarios where average land use per person is unrealistically increased by a factor of 4 to 8 above published estimates. Our results falsify the hypothesis that humans are responsible for the late Holocene CO_2 increase and that anthropogenic land use prevented a new ice age.

1 Introduction

The reconstructed increase in atmospheric CO_2 and CH_4 during the last 8000 years (yr) has stimulated a debate about the underlying causes and mechanisms (e.g., Indermühle et al., 1999; Broecker et al., 2001; Brovkin et al., 2002; Joos et al., 2004; Elsig et al., 2009). Anthropogenic land use change (LUC) has been propounded as a contributing factor. Clearing of natural vegetation for agriculture begins with the first neolithic settlements some ten thousand years before present (Williams, 2000). Even long before industrialisation, anthropogenic land use change could have affected climate and atmospheric chemistry through (i) emissions of carbon and the resulting changes in radiative forcing, (ii) changes in the local albedo and the hydrological balance, and (iii) changes in the emissions of non-CO_2 greenhouse agents, carbon monoxide, and volatile organic carbon compounds (Betts et al., 2007; Bonan, 2008).

Ruddiman (2003, 2007) attributed the observed 20 ppmv increase in atmospheric CO_2 after 8 ka BP to agricultural activities and an assumed climate-carbon cycle feedback. This "early anthropogenic" hypothesis is not supported by published estimates of anthropogenic carbon emissions prior to the industrial period (Joos et al., 2004; Strassmann et al., 2008) and simulated airborne fractions, which are both too low to explain the observed trend and imply a smaller anthropogenic impact. In simulations by Pongratz et al. (2009b), LUC did not cause an increase of atmospheric CO_2 above natural variability before late medieval times, with an average preindustrial airborne fraction of LUC emissions of 21% (800–1850 AD). Inverse modelling based on recently published high resolution $\delta^{13}C$ measurements on the Antarctic Dome C ice core constrains the net contribution of Holocene changes in terrestrial carbon storage to the observed CO_2 rise to 36±37 GtC or 3 ppmv since 5 ka BP (Elsig et al., 2009). Likewise, this result cannot be reconciled with the early anthropogenic hypothesis. However, a hypothetical, extensive early LUC-related carbon source and its associated CO_2 – and $\delta^{13}C$ signal could be masked by a correspondingly large and unaccounted for biogenic sink, such as peat buildup (MacDonald et al., 2006). This leaves a range of possible LUC histories and requires the implementation of explicit LUC scenarios in terrestrial carbon cycle models to further constrain the human impact on atmospheric CO_2 .

The evolution of LUC in the Holocene is uncertain (Kaplan et al., 2009), and so are its impacts on terrestrial carbon stocks, atmospheric CO_2, and climate. Direct historical or archeological information is scarce, and spatial extrapolation of proxy records from natural archives to a global scale remains challenging. Thus, the HYDE 3.1 land use

(LU) reconstruction (Klein Goldewijk, 2001; Klein Goldewijk and van Drecht, 2006), as well as the similar reconstruction of Pongratz et al. (2008), rely on population maps as a proxy for agricultural areas and the simplistic assumption that the agricultural land area required to support a given population is constant (land area per person, LAP).

The assumption of a constant LAP is questionable and – given the assumption of a generally decreasing trend in LAP throughout the Holocene – may lead to an underestimation of the area affected by preindustrial land use and of early LUC-related CO_2 emissions and atmospheric CO_2 changes. Ruddiman and Ellis (2009) argued that this reopens the case of their early anthropogenic hypothesis.

Various lines of evidence indeed point towards a low bias of the above mentioned land use estimates. Kaplan et al. (2009) analyze historical data on population density and forest cover for several European countries. They derive an expression in which LAP is a function of population *density* and thus changes with time. According to their reconstruction of European land use back to 1000 BC, the European landscape was dominated by humans already two thousand years ago, and by 1000 AD, deforested areas covered more than 70% of the land in much of Western Europe. Pollen analyses and historical work (e.g., Soepboer et al., 2010; Williams, 2000) are in line with this result. A historical study by Murphey (1983) reports an even stronger human impact on forests in Medieval China than in Europe. A limited set of low resolution charcoal accumulation records from soils and lacustrine sediments was interpreted as an indication of considerable deforestation after 2000 BP also in the Americas (Nevle and Bird, 2008). However, the comprehensive study by Marlon et al. (2009) suggests that fire frequency and charcoal production during the last millennium covaries with climate rather than population.

The HYDE and Pongratz et al. (2008) reconstructions disagree with the notion of extensive preindustrial deforestation in Europe and other parts of the world. Their assumption of a constant LAP yields a relatively small extent of permanently cultivated areas in all of the above mentioned regions before 1000 AD.

The amount of cultivated land at any time is the net result of land use transitions (clearing and abandonment), which are not specified in, e.g., HYDE 3.1. Hurtt et al. (2006) developed spatio-temporal datasets of land use transitions from the land use maps by Klein Goldewijk (2001) (HYDE version 2) and Ramankutty and Foley (1999), using data on wood harvest and assumptions on land use preferences across the world. This product captures land use patterns such as shifting cultivation and wood harvest, albeit with large uncertainty. In simulations with a dynamic land model, these processes increase land carbon loss over the last 300 yr by up to 50% (Shevliakova et al., 2009). At earlier times, this impact might have been even larger (Olofsson et al., 2008). Still, shifting cultivation, wood harvest, forest management, and their impact on the terrestrial carbon cycle are not captured in many studies (e.g. Strassmann et al., 2008; Pongratz et al., 2008).

The low bias stemming from the neglection of variations in LAP and the effect of shifting cultivations, and the discrepancies between different land use estimates leave a high uncertainty in estimates for historical LUC emissions and preclude a precise quantification of the preindustrial human impact on the carbon cycle at this point. Earlier studies have not addressed this uncertainty. In addition, they are restricted to the past millennium (Brovkin et al., 2006; Pongratz et al., 2009b), assess only the total cumulative carbon emissions before industrialization (Joos et al., 2004; Strassmann et al., 2008), or are of highly qualitative nature (Ruddiman, 2003, 2007; Williams, 2000; Nevle and Bird, 2008).

Here, we present the first transient simulations of the impact of preindustrial land use change on atmospheric CO_2 throughout the Holocene, including an assessment of uncertainty in the evolution of land use.

The Bern Carbon Cycle-Climate Model (BernCC) is forced by explicitly prescribing the evolution of croplands, pastures, and urban areas over the past 12 kyr. As a standard scenario we use the HYDE 3.1 reconstruction. The extent of a possible low bias in the HYDE data and in the simulated impact on the carbon cycle is constrained using three complementary, idealized land use scenarios. The plausible range is explored using a scenario with preindustrial land use extent scaled by a factor of two. Sensitivity to extreme preindustrial deforestation is analyzed using two scenarios that approach the present scale of global land use before or in the first millenium AD. The plausibility of the scenarios is assessed by comparing their LAP with values proposed in the literature. In addition, we check whether the land use scenarios are consistent with the carbon budget of the last millennium as inferred from a single deconvolution analysis (Siegenthaler and Oeschger, 1987).

2 Methods

2.1 Land use scenarios

Four different LUC histories were used (Figs. 1 and 2). The scenarios are identical with respect to the LU area in 10 000 BC and 2005 AD. This is motivated by the assumption that permanent agriculture was practically not existent in 10 000 BC and by the relatively high quality of present-day data. The standard scenario (HY) is defined by the spatially aggregated HYDE 3.1 data (Klein Goldewijk, 2001; Klein Goldewijk and van Drecht, 2006). The spatial aggregation for the application in the BernCC modelling framework ($3.75^\circ \times 2.5^\circ$ spatial resolution) is described in (Strassmann et al., 2008). The HYDE land use data defines the relative share of croplands, pastures and urban areas in each gridcell and at 58 time steps between 10 000 BC and 2005 AD. The temporal resolution varies from millennial before 0 AD, to centennial until 1700 AD and decadal thereafter. HYDE uses a LAP pattern which is roughly constant throughout the entire preindustrial Holocene. Thus, regional LU is directly proportional to regional population as long as unused land is available and uncertainties in population numbers are propagated to estimated LU areas. An average value for LAP can be derived by dividing the global LU area by the global population number (Klein Goldewijk, 2001; Klein Goldewijk and van Drecht, 2006); this yields 1.0–1.3 ha/pers. (hectares per person) (see also Table 2).

In scenario H2, agricultural areas from HYDE are scaled by a factor of 2 before

1700 AD. After 1700, the scaling factor linearly decreases to 1 until 2005 AD. H2 represents a high, but plausible LU scenario with higher preindustrial land use areas than the maximum scenario presented by Pongratz et al. (2008). In H2, up to 70% of the land area is under anthropogenic use in Europe by 1000 AD compared to about 40% in the HY scenario. European LU areas in H2 are roughly in line with the reconstruction of Kaplan et al. (2009). The potential enhancement of emissions due to shifting cultivation by about 50% relative to HY (Shevliakova et al., 2009) is also within the range of H2 (see Sect. 3).

In the extreme scenario X1, all LU areas from 10 000 to 1000 BC are scaled with a factor of 8. This value is derived from the time-dependent relation between population density and the area fraction of agricultural areas in a gridcell, as defined by Eq. (1) in Kaplan et al. (2009) (see Stocker, 2009). After 1000 BC, the areas are linearly interpolated to the 2005 AD distribution of HY. In X1, the pattern of land use areas is identical to HY before 1000 BC. Thereafter, the spatial pattern of HYDE in 2005 AD becomes increasingly visible as a consequence of the linear interpolation between the distribution at 1000 BC and the HYDE distribution at 2005. This implies large areas under agricultural use in X1 already at an early stage and in regions that are unaffected by early human land use in HY. In the illustrative extreme scenario X2, agricultural areas are interpolated between 10 000 BC (zero land use) and the state defined by the HYDE 2005 AD map. Thus, the spatial distribution corresponds to HYDE in 2005 at all times and accordingly, anthropogenic LUC occurs worldwide over the entire Holocene.

To limit the share of total land use to 100%, the LU area according to the above scenario definitions had to be reduced for some cells. In doing so, the relative share of pastures, croplands, and urban areas, as given in HYDE, was conserved. This affected the total land use area only slightly (Fig. 1).

Implicitly assumed global mean LAP values range from 1.3 and 2.5 in HY and H2, respectively to 32 ha/pers. in X2 at 1000 BC. While the HY value is considerably lower than estimates proposed by other authors (see Table 2), X2 exceeds these values by almost an order of magnitude. Also, global mean LAP of X1 in 1000 AD (12 ha/pers.)

is considerably larger than the 4 ha/pers. proposed for European neolithic settlements (Gregg, 1988). Global population numbers for the time before 1000 AD differ by a factor of up to 2 (Pongratz et al., 2008). Thus, LAP of X1 and X2 is considerably larger than published estimates even when taking into account the uncertainties in population. In brief, our LUC scenarios span the wide range from a scenario potentially underestimating preindustrial land use activities (HY) to a scenario with an unrealistically high magnitude and worldwide extent of anthropogenic land use in the Holocene.

2.2 Model description and setup

The land use simulations are performed with the BernCC model (Joos et al., 2001; Strassmann et al., 2008). BernCC is a simplified Earth system model, which includes the Lund-Potsdam-Jena Dynamical Global Vegetation Model (LPJ-DGVM, Sitch et al. (2003)) with a land use component by Strassmann et al. (2008). LPJ simulates terrestrial carbon assimilation and respiration in response to variations in CO_2 and climate. It exchanges net carbon fluxes with a well-mixed atmosphere and a Mixed-Layer Pulse-Response representation of the HILDA ocean model (Joos et al., 1996), which also parametrizes carbonate-sediment interactions (Joos et al., 2004). The coupled modelling framework simulates the evolution of atmospheric CO_2 and climate at low computational costs.

In an earlier study that considered climatic variations on the millennial time scale but no explicit representation of LUC, terrestrial carbon storage increased by 820 to 850 GtC over the past 20 kyrs, and by 28 to 75 GtC over the past 6 kyrs (Joos et al., 2004). These effects are largely independent of LUC-related effects, as ascertained with simulations driven by variable LUC and natural changes. Here, for simplicity of interpretation, we keep all boundary conditions other than LU constant. We use the Climate Research Unit's (CRU) TS 2.1 climatology from 1900 to 1930 (New et al., 1999; Mitchell and Jones, 2005), present-day land-ice distribution (Peltier, 1994; Joos et al., 2004), and the insolation at 1950 AD (Berger, 1978). Emissions of fossil fuel are not included. The CRU climatology is repeated every 31 yr to simulate interannual variability in terrestrial carbon storage.

LUC-related carbon emissions and related changes in atmospheric CO_2 are explicitly modeled by our version of LPJ using a fractional grid cell approach to distinguish different land classes (see Strassmann et al., 2008). Only the net change (difference of deforestation and abandonment) is simulated. After land conversion, carbon from woody biomass is partly released to the atmosphere (25%), the rest is evenly split up and directed to two product pools that decay with turnover times of 2 and 20 yr. The assessment of LUC emissions on a decadal to millennial time scale is not sensitive to the respective values. Carbon from leaves, sapwood and roots enters the litter pools of the appropriate land use area. On agricultural areas, tree plant functional types are suppressed from growing and urban areas are assumed to be void of any biomass.

The model is spun up to equilibrium; model drift in atmospheric CO_2 and carbon inventories is negligible. Simulations are carried out with the standard setup and with suppressed CO_2 fertilization. We distinguish net and primary LU emissions. Primary LU emissions are defined as the net carbon fluxes to the atmosphere in a LU simulation with suppressed fertilization, minus a corresponding simulation without LU. Net emissions differ from primary emissions primarily due to the CO_2 fertilization feedback as defined by Strassmann et al. (2008). Additional feedbacks due to climate variations are implicitly neglected by the setup; the "lost sinks/sources" flux (Strassmann et al., 2008) is small due to the neglection of fossil emissions and the corresponding relatively small variations in CO_2 .

The set of plant functional type-s (PFT) and PFT-specific parameters has been updated from the version by Sitch et al. (2003) as used by Strassmann et al. (2008) and Joos et al. (2004). The new parameters proposed by Wania (2007) are used here in order to achieve a better representation of the vegetation distribution in northern latitudes. In addition, we use a different baseline climatology (CRU TS 2.1 instead of Leemans and Cramer, 1991). These updates reduce the simulated LUC-related carbon emissions over the last 300 yr by about 30% as compared to a simulation based on the original parameters of (Sitch et al., 2003).

2.3 Closing the global carbon budget and the quantification of a residual terrestrial sink

Land use emissions have implications for the budget of atmospheric CO_2 and the stable isotope $^{13}CO_2$, and for the magnitude of carbon sink processes. In turn, the consistency of different land use emissions scenarios with the atmospheric CO_2 and $^{13}CO_2$ evolutions offers an additional means to check the plausibility of land use scenarios. Here, we focus on the CO_2 budget of the last millennium and the 20th century as the earlier millennial-scale Holocene CO_2 variations are influenced by a number of not exactly quantified natural carbon fluxes (e.g. Elsig et al., 2009; Kleinen et al., 2010).

Previous analyses (Joos and Bruno, 1998; Joos et al., 1999; Trudinger et al., 2002; Houghton et al., 2004) of the ice core CO_2 and $^{13}CO_2$ records (Francey et al., 1999) suggest that multi-decadal net ocean-atmosphere and land biosphere-atmosphere fluxes were relatively small (<0.2 GtC yr^{-1}) during the preindustrial millennium and that the net flux from the land biosphere to the atmosphere is comparable to land use emissions estimated by Houghton (2003) for the 19th century. In contrast, a residual sink flux on the order of 1 to 2 GtC yr^{-1} is required to close the CO_2 budget over the more recent decades (Denman et al., 2007); this residual sink flux is linked to the land biosphere and to processes such as unaccounted vegetation regrowth in northern mid-latitudes and stimulation of photosynthesis on land by elevated atmospheric CO_2 and nitrogen input into terrestrial systems (Prentice et al., 2001; Denman et al., 2007). The intention is then not only to check the plausibility of the land use scenarios, but also to address the implications of different plausible preindustrial land use scenarios for the late 20th century residual carbon sink flux.

Technically, we follow the single deconvolution approach of Siegenthaler and Oeschger (1987) and consider the CO_2 budget only. This is permissible as analyses of the combined CO_2 and $^{13}CO_2$ yield very similar results for the last millennium (Joos et al., 1999). The net atmosphere-to-land biosphere flux, $F_{ab,net}$, is taken from Joos et al. (1999). It is quantifed by taking the difference from reconstructed changes

BGD

7, 921–952, 2010

in atmospheric CO_2 (Etheridge et al., 1996; Keeling et al., 1993; Keeling and Whorf, 2003), dN_a/dt, carbon emission from fossil fuels and cement production (Marland et al., 2006), E_{foss}, and the net atmosphere-to-sea flux, $F_{\text{as,net}}$ as computed under prescribed CO_2 with the BernCC model:

$$F_{\text{ab,net}} = -\frac{d}{dt}N_a + E_{\text{foss}} - F_{\text{as,net}} \tag{1}$$

The residual terrestrial sink, F_{sink} is then as in Denman et al. (2007) given by the primary carbon emissions by land use and land use changes, E_{LUC}, and the net flux into the biosphere:

$$F_{\text{sink}} = E_{\text{LUC}} + F_{\text{ab,net}} \tag{2}$$

Uncertainties (1-sdv) in the sink flux related to uncertainties in the ocean model, in fossil emission estimates, and in the ice core CO_2 data have been estimated to be about 0.2 GtC yr^{-1} for the period from 1800 to 1960 (Bruno and Joos, 1997).

3 Results

Cumulative net land use emissions between 10 000 BC and 2004 AD add up to roughly 120 GtC in all scenarios (Fig. 1). Differences of less than 10 GtC occur due to differences in simulated CO_2 and the associated fertilization feedback and in the size of the product pools towards the end of the simulation period (see also Fig. 3). The cumulative primary emissions in year 2004, excluding any LUC-related feedback flux, add up to 177, 183, 157, and 153 GtC in HY, H2, X1, and X2, respectively (see Table 1). Until 1850, cumulative net (primary) emissions are 34 (50), 52 (74), 117 (153), and 124 (153) GtC in HY, H2, X1, and X2, respectively. In the extreme X1 and X2 case, the bulk of these emissions is allocated in the preindustrial period.

The evolution of atmospheric CO_2 (Fig. 1, bottom) strongly depends on the LUC scenario, although all scenarios are identical with respect to the pasture and cropland distribution at the end of the simulation period. Until 2004, CO_2 increases by 22.1, 19.8, 8.9 ppmv, and 6.2 ppmv for HY, H2, X1, and X2, respectively. Differences are even more pronounced when looking at the increase since 1850: 16.6, 12.4, −0.1, −0.4 ppmv for HY, H2, X1 and X2, respectively. For the plausible HY and H2 scenarios, the atmospheric CO_2 rise remained below 0.9 and 1.2 ppmv before 0 AD and 1000 AD, respectively (smoothed time series, see Fig. 1, bottom). CO_2 changes remained below 6 ppmv before 0 AD even for the extreme X1 and X2 scenarios. Only slightly larger CO_2 concentrations changes (<7 ppmv) are simulated when CO_2 fertilization is suppressed (Fig. 1, thin lines).

LUC emissions are redistributed between the biosphere, the ocean/sediments and the atmosphere. On millenial time scales, most of the emissions are absorbed by the ocean and ocean-sediment interactions as a consequence of the very well-understood carbonate chemistry and the dynamic mixing to depth. This is documented extensively in the literature (e.g., Joos et al., 1996; Archer et al., 1997; Cao et al., 2009). Only about 14% of an initial perturbation of the preindustrial atmosphere by a (small) carbon input remains airborne when the atmosphere-ocean system has attained a new equilibrium one to two thousand years after the emission. This airborne fraction is further lowered to 6 to 7% on a multi-millennial time scale by ocean-sediment interactions. Consequently, the airborne fraction is low in our simulations (9% to 16%) at preindustrial times for all four scenarios and in simulations with or without biospheric CO_2 fertilization as the time scales over which carbon emissions occur are multi-millennial (Fig. 3).

The airborne fraction depends inter alia on the growth rate of emissions. The higher the growth rate, the higher the airborne fraction. For a high growth rate scenario the share of more recent emissions on total emissions is higher at any given point in time compared to low growth rate scenarios. Less time is effectively available for the ocean and the land to take up excess CO_2 under high growth in emissions. Thus, the airborne fraction is higher in the exponential-like increasing HY and H2 LUC senarios than in the more linear X1 and X2 scenarios. For today, the simulated airborne fraction is 27, 24, 12 and 9% in HY, H2, X1 and X2, respectively. The relatively high airborne fraction in the HY reflects that the bulk of the LUC occurs in the last two centuries in this scenario. On the other hand, scenarios with large early land use activities are associated with a very low airborne fraction.

Next, the atmospheric CO_2 budget and the residual sink is quantified (Fig. 4). The residual sink is close to zero, between 1005 and 1700 AD in all scenarios. Remaining deviations of up to $\pm 0.2\,\mathrm{GtC\,yr^{-1}}$ may be linked to uncertainties in input data and the impact of unaccounted climatic variations on the carbon cycle. The small land use emissions obtained with all four scenarios are compatible with the evolution of CO_2 during this period. The residual sink flux remains also negligible throughout the 19th century in the HY and H2 scenarios. In other words, the land use emissions of these two scenarios are fully compatible with the evolution of atmospheric CO_2 and current process understanding. No additional, unknown carbon flux needs to be invoked to close the carbon budget prior to the 20th century, suggesting that last millennium land use emissions of these two scenarios are of realistic magnitude. In contrast, the X1 and X2 scenarios yield a residual source of carbon of about 70 GtC between 1700 and 1930 AD. This again suggests that the X1 and X2 scenarios are unrealistic.

The magnitude of early land use has, however, implications for the current carbon budget when considering the difference between the two plausible HY and H2 scenarios. H2 implies a smaller terrestrial sink than HY due to slower land conversion rates and associated lower primary emissions during the second part of the 20th century. The average residual sink flux for the 1990s is 1.9 and $1.3\,\mathrm{GtC\,yr^{-1}}$ for the HY and H2 scenarios, respectively. This indicates that the magnitude of the modern residual sink is potentially becoming smaller when revising upward early LUC.

4 Discussion and conclusion

We assess the LUC-related carbon cycle perturbation with transient simulations using the BernCC simplified Earth system model and the HYDE 3.1 data for croplands and pastures since 10 000 BC and a range of idealized scenarios. Our main findings are (i) that preindustrial anthropogenic land use activities had only a minor impact on the Holocene CO_2 evolution and (ii) that a plausible LU scenario with a larger than generally assumed share of pre- versus post-1850 AD LU extent and LUC emissions considerably decreases the postulated residual sink flux in the 20th century.

Uncertainties inherent in the present simulations are linked to uncertainties in the distribution of carbon in living vegetation and soils in the areas affected by anthropogenic land use and to uncertainties in the evolution of agricultural area and management practices. LPJ and BernCC show skills for a range of metrics (Sitch et al., 2003; McGuire et al., 2001; Joos et al., 2001). The carbon inventories simulated by LPJ compare reasonably well with observation-based estimates; a caveat is that peat and permafrost regions are not explicitly simulated. However, this is expected to have only a small effect on the simulated carbon release, as the overlap of LU areas and peatlands is relatively small on the global scale and non-existent for the case of permafrost regions. Ocean uptake rates and capacity for excess CO_2 are well constrained by radiocarbon data and the carbonate chemistry (Müller et al., 2006; Matsumoto et al., 2004).

Simulated cumulative primary emissions until 1850 AD in the HY scenario (50 GtC) compare well with values proposed by other authors (48–57 GtC, DeFries et al., 1999, 64 GtC, Pongratz et al., 2009b) and the study by Strassmann et al. (2008) with a previous version of BernCC. Houghton (2003) estimated a primary net deforestation flux of 156 GtC over 1850 to 2000 AD, comparable to our primary emission estimate 124 GtC for the same period and the HYDE case. The total cumulative primary emission of 180 GtC is comparable to the estimates of Shevliakova et al. (2009) of 161 to 210 GtC for their scenarios without shifting cultivation and forest management. An additional 60 to 80 GtC might have been emitted in response to shifting cultivation and forest management (Shevliakova et al., 2009) – factors not explicitly considered in our study. For the 1980s and 1990s, simulated average primary land use emissions based on the HYDE data are 1.37 and 0.70 GtC yr^{-1}, respectively. This is lower than the estimates from Houghton (2003), but comparable to the estimates from Achard et al. (2002); DeFries et al. (1999); Strassmann et al. (2008); Shevliakova et al. (2009).

Reconstructing land conversion in the Holocene remains challenging and the currently available datasets neglect potentially important effects of human activities on biomass density such as time varying land demand per person, or management practices such as shifting cultivation and wood harvesting. We address the uncertainty of Holocene LUC reconstructions using three additional idealized scenarios with larger preindustrial anthropogenic land use than in HY. The modern land use is the same in all scenarios. The four scenarios span a wide range from plausible (HY, H2) to extreme upper limit scenarios (X1, X2) with respect to the magnitude and global extent of preindustrial anthropogenic land use. The wide scenario range implicitly more than accounts for possible uncertainties related to preindustrial management practices or the modelled carbon inventories in LPJ. Preindustrial (pre-1850 AD) primary emissions are in the range of 50 to 153 GtC. The historical land use scenarios presented by Ruddiman and Ellis (2009) are bracketed by the range of scenarios of this study. The shape of their scenario associated with the highest land use areas resembles the X1 scenario except that land conversion takes place 1 ka later in X1. We thus expect the respective increase in CO_2 to be similar to X1 with a corresponding time shift.

We have assessed the plausibility of our LU scenarios by analyzing the consistency of their LUC emissions with the atmospheric CO_2 budget and by analyzing the consistency of their implied land use area per person (LAP) with values proposed in the literature. Implied preindustrial LAP values in X1 and X2 are incompatibly larger than published estimates (see Table 2). It remains difficult to justify that on average each individual has used each years 10 to 30 ha of land given the limited technological means available at preindustrial times to use this land for food production. Published estimates are up to 4 ha/pers. We thus conclude that these extreme scenarios do not represent plausible evolutions of the extent of agricultural areas in the Holocene.

An analysis of the budget of atmospheric CO_2 over the last millennium (Fig. 4) is used to further constrain the scenario space. Although we technically considered the CO_2

budget only in a so-called single deconvolution, we stress the fact that analyses that consider both the evolution of CO_2 and of its stable carbon isotope ^{13}C yield very similar results for net atmosphere-ocean and atmosphere land fluxes for the last millennium (Joos et al., 1999; Trudinger et al., 2002). The general pattern of a small residual, non-LUC related terrestrial flux before 1900 AD and a significantly increasing terrestrial sink flux thereafter can be expected from the response of the land biosphere to changing environmental conditions (from a near-equilibrium state to increasing CO_2, nitrogen deposition, climatic change and more recent vegetation regrowth, e.g. due to woody encroachment and fire prevention, not accounted for in land use data). HY and H2 are broadly consistent with this temporal pattern and the budget of CO_2 (and implicitly $^{13}CO_2$) is roughly closed before 1900 AD. The residual sink fluxes in the 1980s and '90s (-1.8 and -1.3 GtC yr^{-1} in HY and H2) agrees with the range of -3.8 to -0.3 GtC yr^{-1} given by Denman et al. (2007). This broad pattern is not reproduced by X1 and X2 and a large unexplained terrestrial (non-LUC related) release of >70 GtC between 1700 and 1930 AD is required to close the carbon budget. No processes have been proposed to explain an unknown terrestrial source of this magnitude. This may further indicate that a large-scale early LUC of the extent assumed in X1 and X2 is unrealistic.

The scenarios are identical with respect to the LU areas at 10 000 BC, when agricultural activity was basically non-existent, and the LU areas in 2005 AD as constrained by satellite observations and surveys. This implies differences in the *timing* and the *rate* of LUC-related carbon emissions, while cumulative emissions converge at roughly the same amount by today. This in turn implies differences in airborne fraction, the atmospheric CO_2 increase, and in the split of emission between periods. Results based on the HYDE reconstruction suggest a split of 28 vs. 72% for pre-1850 vs. post-1850 primary emissions. Olofsson et al. (2008), who explicitly account for the marginal but wide-spread impact of shifting cultivation and longer fallow periods of croplands in earlier agricultural systems, suggest a much higher share of pre-1850 emissions (43%). This is close to the respective split in H2 (40%).

The split of emissions has important consequences for the CO_2 increase and residual sink flux. The standard scenario (HY) is associated with the highest CO_2 increase and airborne fraction by 2004 AD. Doubling agricultural areas in 1700 AD (H2 scenario) yields a reduction of the CO_2 increase since 1700 AD by 20% and since 1850 AD by 25% relative to the standard scenario. The comparatively low preindustrial anthropogenic land use assumed in the HYDE data, implies in turn large land use area changes over the industrial period. This might point to a tendency to overestimate the LUC-induced CO_2 increase over the industrial period in simulations forced by the HYDE land use data.

The difference between the residual sink fluxes of HY and H2 increases from less than 0.1 GtC yr^{-1} before 1900 AD to 0.46 GtC yr^{-1} at present. This difference, which stems from different, allegedly plausible LU reconstructions, is much smaller than the total uncertainty of the residual sink flux (−4.3 to −0.9 GtC yr^{-1}) as given by Denman et al. (2007). Still, it leaves a considerable uncertainty in this flux and prevents us to draw further conclusions about the absolute magnitude of this sink. However, our results suggest that an upward revision of the ratio between preindustrial versus industrial LUC as in the H2 scenario tend to reduce the modern residual terrestrial sink flux by the order of half a GtC yr^{-1}. This may help to reconcile the modern carbon budget as it appears difficult to explain current upper bound estimates of the residual sink flux mechanistically and consistently with bottom-up estimates of land carbon fluxes (Denman et al., 2007).

The contribution of anthropogenic land use activities to the last millennium CO_2 evolution is noticeable and overall about 4 ppmv for the period 1000 AD to 1850 in the HY and H2 scenarios. This is relevant when it comes to explain the small last millennium CO_2 trends or to infer carbon cycle-warming feedbacks from reconstructed CO_2 and temperature (Gerber et al., 2003; Frank et al., 2010).

Preindustrial anthropogenic land use has only marginally contributed to the Holocene CO_2 rise of 20 ppmv. Even in the extreme X2 scenario and without considering a potential CO_2 fertilization, atmospheric CO_2 increased by less than 8 ppmv over the past 8 ka. Primary emissions related to anthropogenic land use before 1000 AD are 9 and

18 GtC in the more plausible HY and H2 scenarios and atmospheric CO_2 increases by less than 1.2 ppmv until 1000 AD in H2. The conclusion of a small Holocene CO_2 increase due to anthropogenic land use is robust with respect to the choice of scenario and with respect to CO_2-fertilization, albedo changes, and climate-carbon cycle feedbacks. Allocating land use activities earlier in time causes a smaller CO_2 increase in the atmosphere as the ocean-sediment system has more time to absorb excess CO_2. Simulations with suppressed CO_2 fertilization yield only marginally higher atmospheric CO_2 levels. Holocene CO_2 changes are primarily driven by natural processes such as changes in the ocean calcium carbonate cycle and natural terrestrial carbon stock changes (Elsig et al., 2009; Kleinen et al., 2010).

The radiative forcing related to an increase in CO_2 of 8 ppmv as found for the extreme X2 scenario is 0.1 Wm^{-2} only. An additional 0.1 Wm^{-2} forcing is computed under the extreme assumptions that all the Holocene CH_4 and N_2O changes are related to human land use. Together these forcings imply a warming of merely 0.16 to 0.35 °C (for a nominal climate sensitivity of 2 to 4.5 °C for doubling CO_2) and a carbon cycle-warming feedback on the order of 2 ppmv (Frank et al., 2010). The pronounced albedo increase of deforestation in the mid-latitudes (Betts et al., 2007) counteracts these biogeochemical forcings by as much as −0.2 Wm^{-2} for the present-day land use (IPCC, 2007) and by about −0.05 Wm^{-2} for the pre-1800 AD state (Pongratz et al., 2009a). Combining the CO_2 effect and the albedo forcing of historical land use change even results in a slight cooling (Brovkin et al., 2006). The notion reiterated in several papers (Ruddiman, 2003; Ruddiman and Ellis, 2009) that antropogenic land use caused CO_2 to rise, climate to warm, and thereby prevented a new ice age is not tenable. Inverse top-down as well as bottom up studies like this one come to the same conclusion (Joos et al., 2004; Broecker and Stocker, 2006; Claussen et al., 2005; Elsig et al., 2009; Strassmann et al., 2008).

We emphasize the unresolved uncertainties of preindustrial land use reconstructions. More elaborate LUC reconstructions which account for the most important characteristics of agricultural development in the Holocene and during the last millennium (spatio-temporal evolution of LAP, shifting cultivation, wood harvesting and wet rice agriculture) will be needed to refine the estimates of LUC-related carbon emission and the biogeophysical forcing, and of the contemporary residual terrestrial sink and to address the human impact on the methane cycle.

Acknowledgements. We thank H. Fischer and R. Spahni for comments. We appreciate support by the Swiss National Science Foundation through the National Centre of Competence in Research (NCCR) Climate and by the European Commission through the FP7 project Past4Future (grant no. 243908).

References

Achard, F., Eva, H. D., Stibig, H. J., Mayaux, P., Gallego, J., Richards, T., and Malingreau, J. P.: Determination of deforestation rates of the world's humid tropical forests, Science, 297, 999–1002, 2002. 935

Archer, D., Keshgi, H., and Maier-Reimer, E.: Multiple timescales for neutralization of fossil fuel CO_2, Geophys. Res. Lett., 24, 405–408, 1997. 932

Berger, A.: Long-term variations of daily insolation and Quaternary climatic changes, J. Atmos. Sci., 35, 2362–2367, 1978. 928

Betts, R. A., Falloon, P. D., Goldewijk, K. K., and Ramankutty, N.: Biogeophysical effects of land use on climate: Model simulations of radiative forcing and large-scale temperature change, Agr. Forest. Meteorol., 142, 216–233, 2007. 923, 938

Bonan, G. B.: Forests and Climate Change: Forcings, Feedbacks, and the Climate Benefits of Forests, Science, 320, 1444–1449, doi:10.1126/science.1155121, 2008. 923

Broecker, W. S. and Stocker, T. F.: The Holocene CO_2 rise: anthropogenic of natural?, EOS, 87, 27–29, 2006. 938

Broecker, W. S., Lynch-Stieglitz, J., Clark, E., Hajdas, I., and Bonani, G.: What caused the atmosphere's CO_2 content to rise during the last 8000 years?, Geochem. Geophy. Geosy., 2, doi:2001GB000177, 2001. 922

Brovkin, V., Bendtsen, J., Claussen, M., Ganopolski, A., Kubatzki, C., Petoukhov, V., and Andreev, A.: Carbon cycle, vegetation, and climate dynamics in the Holocene: Experiments with

the CLIMBER-2 model, Global Biogeochem. Cy., 16, 1139, doi:10.1029/2001GB001662, 2002. 922
Brovkin, V., Claussen, M., Driesschaert, E., Fichefet, T., Kicklighter, D., Loutre, M., Matthews, H., Ramankutty, N., Schaeffer, M., and Sokolov, A.: Biogeophysical effects of historical land cover changes simulated by six Earth system models of intermediate complexity, Clim. Dynam., 26, 587–600, 2006. 925, 938
Bruno, M. and Joos, F.: Terrestrial carbon storage during the past 200 years: A Monte Carlo Analysis of CO_2 data from ice core and atmospheric measurements, Global Biogeochem. Cy., 11, 111–124, 1997. 931
Cao, L., Eby, M., Ridgwell, A., Caldeira, K., Archer, D., Ishida, A., Joos, F., Matsumoto, K., Mikolajewicz, U., Mouchet, A., Orr, J. C., Plattner, G.-K., Schlitzer, R., Tokos, K., Totterdell, I., Tschumi, T., Yamanaka, Y., and Yool, A.: The role of ocean transport in the uptake of anthropogenic CO_2, Biogeosciences, 6, 375–390, 2009, http://www.biogeosciences.net/6/375/2009/. 932
Claussen, M., Brovkin, V., Calov, R., Ganopolski, A., and Kubatzki, C.: Did humankind prevent a Holocene glaciation?, Climatic Change, 69, 409–417, 2005. 938
DeFries, R. S., Field, C. B., Fung, I., Collatz, G. J., and Bounoua, L.: Combining satellite data and biogeochemical models to estimate global effects of human-induced land cover change on carbon emissions and primary productivity, Global Biogeochem. Cy., 13, 803–815, 1999. 934, 935, 947
Denman, K. L., Brasseur, G., Chidthaisong, A., Ciais, P., Cox, P., Dickinson, R. E., Hauglustaine, D., Heinze, C., Holland, E., Jacob, D., Lohmann, U., Ramachandran, S., da Silva Dias, P. L., Wofsy, S. C., and Zhang, X.: Chapter 7: Couplings Between Changes in the Climate System and Biogeochemistry, in: Climate Change 2007: The Physical Science Basis. Contribution of Working Group I to the Fourth Assessment Report of the Intergovernmental Panel on Climate Change, edited by: Solomon, S., Qin, D., Manning, M., Chen, Z., Marquis, M., Averyt, K., Tignor, M., and Miller, H., Cambridge Univ. Press, United Kingdom and New York, NY, USA, 2007. 930, 931, 936, 937
Elsig, J., Schmitt, J., Leuenberger, D., Schneider, R., Eyer, M., Leuenberger, M., Joos, F., Fischer, H., and Stocker, T. F.: Stable isotope constraints on Holocene carbon cycle changes from an Antarctic ice core, Nature, 461, 507–510, 2009. 922, 923, 930, 938
Etheridge, D. M., Steele, L. P., Langenfelds, R. L., Francey, R. J., Barnola, J., and Morgan, V. I.: Natural and anthropogenic changes in atmospheric CO_2 over the last 1000 years from air

in Antarctic ice and firn, J. Geophys. Res., 101, 4115–4128, doi:10.1029/95JD03410, 1996. 931

Francey, R. J., Allison, C. E., Etheridge, D. M., Trudinger, C. M., Enting, I. G., Leuenberger, M., Langenfelds, R. L., Michel, E., and Steele, L. P.: A 1000-year high precision record of $\delta^{13}C$ in atmospheric CO_2, Tellus B, 51, 170–193, doi:10.1034/j.1600-0889.1999.t01-1, 1999. 930

Frank, D. C., Esper, J., Raible, C. C., Büntgen, U., Trouet, V., Stocker, B., and Joos, F.: Ensemble reconstruction constraints of the global carbon cycle sensitivity to climate, Nature, 463, 527–530, 2010. 937, 938

Gerber, S., Joos, F., Brügger, P., Stocker, T. F., Mann, M. E., Sitch, S., and Scholze, M.: Constraining temperature variations over the last millennium by comparing simulated and observed atmospheric CO_2, Clim. Dynam., 20, 281–299, doi:10.1007/s00382-002-0270-8, 2003. 937

Gregg, S. A.: Foragers and Farmers: Population Interaction and Agricultural Expansion in Prehistoric Europe, Prehistoric Archeology and Ecology Series, Chicago, 1988. 928, 948

Houghton, R. A.: Revised estimates of the annual net flux of carbon to the atmosphere from changes in land use and land management 1850–2000, Tellus, 55B, 378–390, 2003. 930, 934, 935, 947

Houghton, R. A., Joos, F., and Asner, G. P.: The effects of land use and management on the global carbon cycle, in: Land Change Science Observing, Monitoring and Understanding Trajectories of Change on the Earth's Surface, edited by: Turner, I. I., Gutman, G., Janetos, A. C., Justice, C. O., Moran, E. F., Mustard, J. F., Rindfuss, R. R., Skole, D., and Cochrane, M. A., Kluwer Academic Publishers, Dordrecht, The Netherlands, 2004. 930

Hurtt, G. C., Frolking, S., Fearon, M. G., Moore, B., Shevliakova, E., Malyshev, S., Pacala, S. W., and Houghton, R. A.: The underpinnings of land-use history: three centuries of global gridded land-use transitions, wood-harvest activity, and resulting secondary lands, Glob. Change Biol., 12, 1208–1229, doi:10.1111/j.1365-2486.2006.01150.x, 2006. 925

Indermühle, A., Stocker, T. F., Joos, F., Fischer, H., Smith, H. J., Wahlen, M., Deck, B., Mastroianni, D., Tschumi, J., Blunier, T., , R., and Stauffer, B.: Holocene carbon-cycle dynamics based on CO_2 trapped in ice at Taylor Dome, Antarctica, Nature, 398, 121–126, doi:10.1038/18158, 1999. 922

IPCC: Summary for Policymakers, in: Climate Change 2007: The Physical Science Basis. Contribution of Working Group I to the Fourth Assessment Report of the Intergovernmental Panel on Climate Change, edited by: Solomon, S., Qin, D., Manning, M., Chen, Z., Marquis,

BGD

7, 921–952, 2010

Holocene land use and CO_2

B. Stocker et al.

M., Averyt, K., Tignor, M., and Miller, H., Cambridge Univ. Press, United Kingdom and New York, NY, USA, 2007. 938

Joos, F. and Bruno, M.: Long-term variability of the terrestrial and oceanic carbon sinks and the budgets of the carbon isotopes ^{13}C and ^{14}C, Global Biogeochem. Cy., 12, 277–295, 1998. 930

Joos, F., Bruno, M., Fink, R., Stocker, T. F., Siegenthaler, U., Le Quéré, C., and Sarmiento, J. L.: An efficient and accurate representation of complex oceanic and biospheric models of anthropogenic carbon uptake, Tellus, 48B, 397–417, 1996. 928, 932

Joos, F., Meyer, R., Bruno, M., and Leuenberger, M.: The variability in the carbon sinks as reconstructed for the last 1000 years, Geophys. Res. Lett., 26, 1437–1440, 1999. 930, 936, 952

Joos, F., Prentice, I. C., Sitch, S., Meyer, R., Hooss, G., Plattner, G.-K., Gerber, S., and Hasselmann, K.: Global warming feedbacks on terrestrial carbon uptake under the Intergovernmental Panel on Climate Change (IPCC) emission scenarios, Global Biogeochem. Cy., 15, 891–907, 2001. 928, 934

Joos, F., Gerber, S., Prentice, I. C., Otto-Bliesner, B. L., and Valdes, P. J.: Transient simulations of Holocene atmospheric carbon dioxide and terrestrial carbon since the Last Glacial Maximum, Global Biogeochem. Cy., 18, 1–18, doi:10.1029/2003GB002156, 2004. 922, 923, 925, 928, 929, 938

Kaplan, J., Krumhardt, K., and Zimmermann, N.: The prehistoric and preindustrial deforestation in Europe, Quaternary Sci. Rev., 28, 3016–3034, 2009. 923, 924, 927

Keeling, C. D. and Whorf, T. P.: Atmospheric CO_2 records from sites in the SIO air sampling network, in: Trends: A Compendium of Data on Global Change, Carbon Dioxide Information Analysis Center, Oak Ridge National Laboratory, US Department of Energy, Oak Ridge, Tenn., USA, 2003. 931

Keeling, R., Najjar, R. P., Bender, M. L., and Tans, P. P.: What atmospheric oxygen measurements can tell us about the global carbon cycle, Global Biogeochem. Cy., 7, 37–67, 1993. 931

Klein Goldewijk, K.: Estimating global land use change over the past 300 years: The HYDE Database, Global Biogeochem. Cy., 15, 417–433, 2001. 924, 925, 926, 948

Klein Goldewijk, K. and van Drecht, G.: HYDE3: Current and historical population and land cover, in: Integrated modelling of global environmental change. An overview of IMAGE 2.4., edited by Bouwman, A. F., Kram, T., and Klein Goldewijk, K., Netherlands Environmental

Assessment Agency (MNP), Bilthoven, The Netherlands, 2006. 924, 926, 948

Kleinen, T., Brovkin, V., von Bloh, W., Archer, D., and Munhoven, G.: Holocene carbon cycle dynamics, Geophys. Res. Lett., 37, L02705, doi:10.1029/2009GL041391, 2010. 930, 938

Leemans, R. and Cramer, W.: The IIASA climate database for land areas on a grid with 0.5° resolution. Research Report RR -91-18., Tech. rep., International Institute for Applied System Analysis, 1991. 929

MacDonald, G. M., Beilman, D. W., Kremenetski, K. V., Sheng, Y., Smith, L. C., and Velichko, A. A.: Rapid Early Development of Circumarctic Peatlands and Atmospheric CH_4 and CO_2 Variations, Science, 314, 285–288, doi:10.1126/science.1131722, 2006. 923

Marland, G., Boden, T. A., and Andres, R. J.: Global, Regional, and National CO_2 Emissions, in: Trends: A Compendium of Data on Global Change, Carbon Dioxide Information Analysis Center, Oak Ridge National Laboratory, US Department of Energy, Oak Ridge, Tenn., USA, 2006. 931

Marlon, J. R., Bartlein, P. J., Carcaillet, C., Gavin, D. G., Harrison, S. P., Higuera, P. E., Joos, F., Power, M. J., and Prentice, I. C.: Climate and human influences on global biomass burning over the past two millennia, Nature Geosci., 2, 307–307, 2009. 924

Matsumoto, K., Sarmiento, J. L., Key, R. M., Aumont, O., Bullister, J. L., Caldeira, K., Campin, J.-M., Doney, S. C., Drange, H., Dutay, J.-C., Follows, M., Gao, Y., Gnanadesikan, A., Gruber, N., Ishida, A., Joos, F., Lindsay, K., Maier-Reimer, E., Marshall, J. C., Matear, R. J., Monfray, P., Najjar, R., Plattner, G.-K., Schlitzer, R., Slater, R., Swathi, P. S., Totterdell, I. J., Weirig, M.-F., Yamanaka, Y., Yool, A., and Orr, J. C.: Evaluation of ocean carbon cycle models with data-based metrics, Geophys. Res. Lett., 31, 31, L07303, doi:10.1029/2003GL018970, 2004. 934

McGuire, A. D., Sitch, S., Clein, J. S., Dargaville, R., Esser, G., Foley, J., Heimann, M., Joos, F., Kaplan, J., Kicklighter, D. W., Meier, R. A., Melillo, J. M., Moore III, B., Prentice, I. C., Ramankutty, N., Reichenau, T., Schloss, A., Tian, H., Williams, L. J., and Wittenberg, U.: Carbon balance of the terrestrial biosphere in the twentieth century: Analyses of CO_2, climate and land use effects with four process-based ecosystem models, Global Biogeochem. Cy., 15, 183–206, 2001. 934

Mitchell, T. D. and Jones, P. D.: An improved method of constructing a database of monthly climate observations and associated high-resolution grids, Int. J. Climatol., 25, 693–712, doi:10.1002/joc.1181, 2005. 928

Monnin, E., Indermuhle, A., Dallenbach, A., Fluckiger, J., Stauffer, B., Stocker, T. F., Raynaud, D., and Barnola, J.-M.: Atmospheric CO_2 Concentrations over the Last Glacial Termination, Science, 291(5501), 112–114, 2001. 949

Müller, S. A., Joos, F., Edwards, N. R., and Stocker, T. F.: Water mass distribution and ventilation time scales in a cost-efficient, three-dimensional ocean model, J. Climate, 19, 5479–5499, 2006. 934

Murphey, R.: Deforestation in Modern China, in: Global Deforestation and the Nineteenth Century World Economy, edited by: Tucker, R. P. and Richards, J. F., Duke University Press, Durham, NC, 1983. 924

Nevle, R. J. and Bird, D. K.: Effects of syn-pandenic fire reduction and reforestation in the tropical Americas on atmospheric CO_2 during European conquest, Paleogeogr. Paleocl. Paleoecol., 264, 25–38, 2008. 924, 925

New, M., Hulme, M., and Jones, P.: Representing Twentieth-Century Space-Time Climate Variability. Part I: Development of a 1961-90 Mean Monthly Terrestrial Climatology, J. Climate, 12, 829–856, 1999. 928

Olofsson, Jorgen, Hickler, and Thomas: Effects of human land-use on the global carbon cycle during the last 6,000 years, Vegetation History and Archaeobotany, 17, 605–615, doi:10.1007/s00334-007-0126-6, 2008. 925, 936, 947

Peltier, W. R.: Ice-age paleotopography, Science, 265, 195–201, 1994. 928

Pongratz, J., Reick, C., Raddatz, T., and Claussen, M.: A reconstruction of global agricultural areas and land cover for the last millennium, Global Biogeochem. Cy., 22, GB3018, doi:10.1029/2007GB003153, 2008. 924, 925, 927, 928

Pongratz, J., Raddatz, T., Reick, C. H., Esch, M., and Claussen, M.: Radiative forcing from anthropogenic land cover change since AD 800, Geophys. Res. Lett., 36, L02709, doi:10.1029/2008GL036394, 2009a. 938

Pongratz, J., Reick, C. H., Raddatz, T., and Claussen, M.: Effects of anthropogenic land cover change on the carbon cycle of the last millennium, Global Biogeochem. Cy., 23, GB4001+, doi:10.1029/2009GB003488, 2009b. 923, 925, 934, 947

Prentice, I. C., Farquhar, G. D., Fasham, M. J., Goulden, M. I., Heimann, M., Jaramillo, V. J., Kheshgi, H. S., LeQuéré, C., Scholes, R. J., and Wallace, D. W. R.: The carbon cycle and atmospheric CO_2, in: Climate Change 2001: The Scientific Basis. Contribution of Working Group I to the Third Assessment Report of the Intergovernmental Panel on Climate Change, edited by: Houghton, J. T., Ding, Y., Griggs, D., Noguer, M., van der Linden, P., Dai, X., Maskell, K., and Johnson, C. A., Cambridge University Press, Cambridge, United Kingdom

BGD

7, 921–952, 2010

Holocene land use and CO_2

B. Stocker et al.

and New York, NY, USA, 183–237, 2001. 930
Ramankutty, N. and Foley, J. A.: Estimating historical changes in global land cover: Croplands from 1700 to 1992, Global Biogeochem. Cy., 13, 997–1027, 1999. 925
Ramankutty, N., Foley, J. A. and Olejniczak, N. J.: People on the land: Changes in global population and croplands during the 20th century, Ambio, 31(3), 251–257, 2002. 948
Ruddiman, W. F.: The anthropogenic greenhouse era began thousands of years ago, Climatic Change, 61, 261–293, 2003. 923, 925, 938
Ruddiman, W. F.: The early anthropogenic hypothesis: Challenges and responses, Rev. Geophys., 45, RG4001+, doi:10.1029/2006RG000207, 2007. 923, 925
Ruddiman, W. F. and Ellis, E. C.: Effect of per-capita land use changes on Holocene forest clearance and CO_2 emissions, Quaternary Sci. Rev., 28, 3011–3015, doi:10.1016/j.quascirev.2009.05.022, 2009. 924, 935, 938, 948
Shevliakova, E., Pacala, S. W., Malyshev, S., Hurtt, G. C., Milly, P. C. D., Caspersen, J. P., Sentman, L. T., Fisk, J. P., Wirth, C., and Crevoisier, C.: Carbon cycling under 300 years of land use change: Importance of the secondary vegetation sink, Global Biogeochem. Cy., 23, GB2022, doi:10.1029/2007GB003176, 2009. 925, 927, 934, 935, 947
Siegenthaler, U. and Oeschger, H.: Biospheric CO_2 emissions during the past 200 years reconstructed by deconvolution of ice core data, Tellus B, 39, 140–154, 1987. 926, 930
Sitch, S., Smith, B., Prentice, I. C., Arneth, A., Bondeau, A., Cramer, W., Kaplan, J. O., Levis, S., Lucht, W., Sykes, M. T., Thonicke, K., and Venevsky, S.: Evaluation of ecosystem dynamics, plant geography and terrestrial carbon cycling in the LPJ dynamic global vegetation model, Glob. Change Biol., 9, 161–185, 2003. 928, 929, 934
Soepboer, W., Sugita, S., and Lotter, A. F.: Modelling regional vegetation changes on the Swiss Plateau during the past two millennia, Quaternary Science Reviews, submitted, 2010. 924
Stocker, B.: Transient simulations of land use change in the Holocene - Separating the human impact from natural drivers of the carbon cycle, Master's thesis, University of Bern, online available at: http://www.climatestudies.unibe.ch/students/theses/msc/17.pdf, 2009. 927
Strassmann, K. M., Joos, F., and Fischer, G.: Simulating effects of land use changes on carbon fluxes: past contributions to atmospheric CO_2 increases and future commitments due to losses of terrestrial sink capacity, Tellus B, 60, 583–603, doi:10.1111/j.1600-0889.2008.00340.x, 2008. 923, 925, 926, 928, 929, 934, 935, 938, 947
Trudinger, C. M., Enting, I. G., Rayner, P. J., and Francey, R. J.: Kalman filter analysis of ice core data 2. Double deconvolution of CO_2 and δ^{13}C measurements, J. Geophys. Res., 107,

4423, doi:10.1029/2001JD001112, 2002. 930, 936
Wania, R.: Modelling northern peatland land surface processes, vegetation dynamics and methane emissi, Ph.D. thesis, University of Bristol, 25 pp., 2007. 929
Williams, M.: Deforesting the Earth - From Prehistory to Global Crisis, University of Chicago Press, Chicago and London, 2000. 923, 924, 925

Table 1. Primary carbon emissions from anthropogenic land use and land use change (in GtC). Comparison of this study's four scenarios (HY, H2, X1, X2) with published results. "Present" is indicated in parentheses for each source; "industrial" refers to the period between 1850 and "present", unless indicated differently. [a] HYDE data, shifting cultivation between 23° N and 23° S; [b] HYDE data, no shifting cultivation.

	until 1850 AD	industrial	until present
HY	50	127	177 (2004)
H2	74	109	183 (2004)
X1	153	4	157 (2004)
X2	153	0	153 (2004)
DeFries et al. (1999)	48-57	125–151	182–199 (1987)
Houghton (2003)		156	
Strassmann et al. (2008)	94	187	284 (2004)
Olofsson et al. (2008)	114	161	148 (1990)
Pongratz et al. (2009b)	63	108	171 (2000)
Shevliakova et al. (2009)[a]		240 (1700-2000)	
Shevliakova et al. (2009)[b]		161 (1700-2000)	

Table 2. Global mean land area per person (LAP, in ha/pers.). The values for the four scenarios are derived by dividing the global LU area of the scenario and the global population as given in Klein Goldewijk (2001); Klein Goldewijk and van Drecht (2006).

	1000 BC	1000 AD	1850 AD
HY	1.3	1.0	1.1
H2	2.5	2.1	1.6
X1	9.5	12	3.7
X2	32	15	3.8
Ramankutty et al. (2002)	0.07–0.35 (20th century)		
Ruddiman and Ellis (2009)	4 (5000 BC); 0.4 (before industrialisation)		
Gregg (1988)	4 (European neolithic settlement)		

BGD

7, 921–952, 2010

Holocene land use and CO_2

B. Stocker et al.

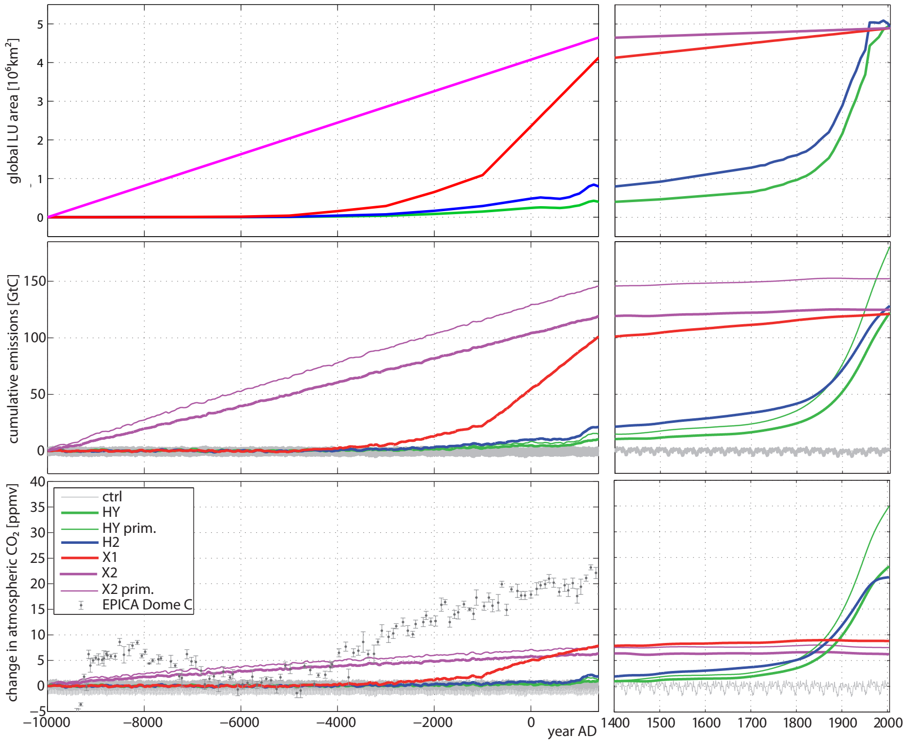

Fig. 1. Evolution of global land use area and land use related carbon emissions and changes in atmospheric CO_2 over the Holocene for four land use scenarios (HY, H2, X1, X2). Top: global total land use area (sum of croplands, pastures and urban). Middle: cumulative net emissions. Bottom: change in atmospheric CO_2 concentration relative to the concentration at the start of the period (263 ppmv). Thin lines indicate primary emissions and corresponding CO_2 increase without the fertilization feedback. CO_2 anomalies relative to 8 ka BP (259 ppmv) measured on the EPICA Dome C ice core (Monnin et al., 2001) are depicted by the grey symbols with 2-σ error bars. Time series of the different scenarios are splined with a cut-off period of 100 yr. The simulated natural interannual variability is illustrated by the light grey band in the lower panels.

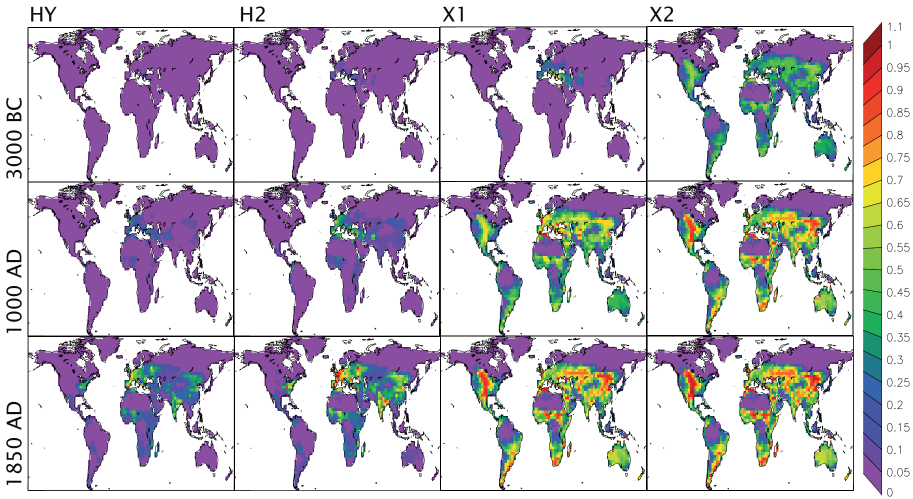

Fig. 2. Area fraction of agricultural land (sum of cropland, pastures and urban) of different scenarios on the aggregated 2.5×3.75° grid used by LPJ. The present-day distribution is congruent with the X2 maps but with larger land use areas.

BGD

7, 921–952, 2010

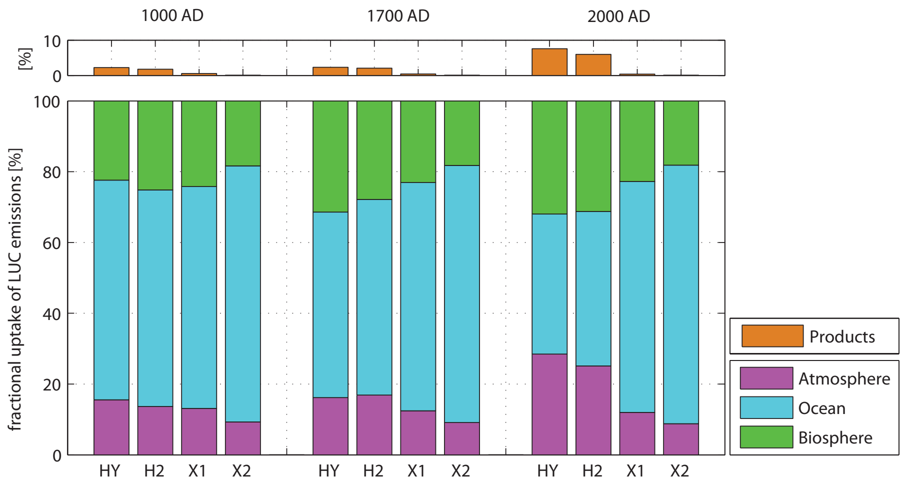

Fig. 3. Simulated redistribution of carbon emissions from land use and land use change between the atmosphere (red), ocean (blue), the land biosphere (green), and product pools (brown) for 1000 AD (left), 1700 AD (middle), and 2000 AD (right) and for four land use scenarios. Values represent fractions in percentage of cumulative emissions, including the delayed emissions from product pools. Values are averages over the 31-year period prior to the labelled year. The uptake by the land biosphere is due to CO_2 fertilisation.

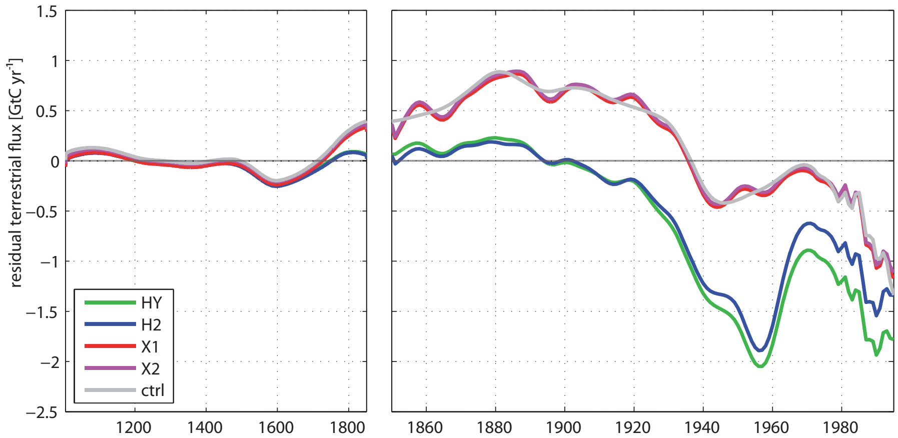

Fig. 4. Residual terrestrial carbon flux over the last millennium for four land use scenarios. Positive values represent a net source. The residual flux is given by the net atmosphere-to-land carbon flux and primary land use emissions. The net atmosphere-to-land flux is derived by a single-deconvolution analysis as described in Joos et al. (1999). Data are splined with a cut-off period of 300 year prior to 1850 AD and 40 year thereafter. For comparison, the residual flux for zero land use emissions is shown by the grey line ("ctrl").